Contents lists available at ScienceDirect

Icarus

Refining the asteroid taxonomy by polarimetric observations

I.N. Belskaya [a,*], S. Fornasier [b], G.P. Tozzi [c], R. Gil-Hutton [d], A. Cellino [e], K. Antonyuk [f], Yu. N. Krugly [a], A.N. Dovgopol [a], S. Faggi [c]

[a] Institute of Astronomy, V.N. Karazin Kharkiv National University, 35 Sumska Str., 61022 Kharkiv, Ukraine
[b] LESIA, Observatoire de Paris, PSL Research University, CNRS, Univ. Paris Diderot, Sorbonne Paris Cité, UPMC Univ., Paris 06, Sorbonne Universités, 5 Place J. Janssen, Meudon Pricipal Cedex 92195, France
[c] INAF – Oss. Astrofisico di Arcetri, Largo E. Fermi 5, I-50125 Firenze, Italy
[d] CASLEO and San Juan National University, Av. España sur 1512, J5402DSP San Juan, Argentina
[e] INAF – Oss. Astrofisico di Torino, via Osservatorio 20, I-10025 Pino Torinese, Italy
[f] Crimean Astrophysical Observatory, 98409 Nauchny, Crimea

ARTICLE INFO

ABSTRACT

We present new results of polarimetric observations of 15 main belt asteroids of different composition. By merging new and published data we determined polarimetric parameters characterizing individual asteroids and mean values of the same parameters characterizing different taxonomic classes. The majority of asteroids show polarimetric phase curves close to the average curve of the corresponding class. We show that using polarimetric data it is possible to refine asteroid taxonomy and derive a polarimetric classification for 283 main belt asteroids. Polarimetric observations of asteroid (21) Lutetia are found to exhibit possible variations of the position angle of the polarization plane over the surface.

© 2016 Elsevier Inc. All rights reserved.

1. Introduction

During the last decade polarimetric techniques have been actively applied to study asteroid surfaces. Long-term observational programs were carried out at the 2.1 m telescope of the Complejo Astronómico El Leoncito (CASLEO) in Argentina (Gil-Hutton et al., 2014), at the 1.25 m telescope of the Crimean Astrophysical Observatory in Ukraine (Belskaya et al., 2009), and at the 1.8 m telescope of the Astrophysical Observatory of Asiago in Italy (Fornasier et al., 2006). The observational surveys were mainly aimed to characterize the polarimetric behavior of asteroids of different composition (Belskaya et al., 2003 , 2005; Fornasier et al., 2006; Gil-Hutton, 2007; Gil-Hutton et al., 2008 , 2014; Gil-Hutton and Cañada-Assandri, 2011 , 2012; Cañada-Assandri et al., 2012).

The linear polarization degree P_r of sunlight scattered by asteroid's surfaces is usually defined in terms of differences between the intensities of the components of the light beam polarized along the planes perpendicular ($I_\perp$) and parallel ($I_{||}$) to the scattering plane:

$$P_r = \frac{I_\perp - I_{//}}{I_\perp + I_{//}}.$$

Using this definition, asteroids (and other asmosphereless Solar System bodies) exhibit a typical dependence $P_r(\alpha)$ of linear polarization upon the phase angle α, characterized by the presence of a negative polarization branch reaching an extreme (negative) value P_{min} at the phase angle α_{min}, and an ascending branch, characterized by an inversion angle α_{inv} at which P_r changes its sign, showing a linear trend characterized by a polarimetric slope h. All these polarimetric parameters are of great interest as they characterize surface physical properties, mainly being related to the geometric albedo and texture.

The interpretation of polarimetric observations of asteroids in terms of physical characteristics of their surfaces is not straightforward. The main conclusions from asteroid polarimetry are mostly based on various empirical relationships (see Belskaya et al., 2015 for a review). It was shown that asteroid's albedo Ag can be derived directly from polarimetric measurements by using the empirical relationship

$$\log(A_g) = C_1 \log(h) + C_2,$$

where the parameters C_1 and C_2 are constants. Such kind of the empirical relationships "albedo – polarimetric slope" and "albedo – P_{min}" have been successfully used to determine asteroid albedos from polarimetric data alone (Zellner and Gradie, 1976; Lupishko and Mohamed 1996; Cellino et al., 1999). Recently Cellino et al. (2015b) made a new analysis of the relationships between the ge-

* Corresponding author.
  E-mail address: Irina@astron.kharkov.ua (I.N. Belskaya).

ometric albedo and polarization parameters of asteroids. They proposed new calibrations and used them to derive polarimetric albedos from re-analysis of published data (Cellino et al., 2015b , 2016).

In this paper we assess the possible role of polarimetry in refining asteroid taxonomy. In the 70s and 80s, values of geometric albedo derived from polarimetry had been used in the derivation of different taxonomic classes, in particular to distinguish between objects exhibiting similar spectro-photometric properties, but quite different albedos (see Tholen and Barucci, 1989 for a review). The insufficient growth of the polarimetric database led subsequently to exclude polarimetric data from the derivation of asteroid taxonomic classes. Later two new analyses were published by Goidet et al. (1995) and Penttilä et al. (2005). They considered polarimetric observations of about 100 asteroids and compared the average phase curves characterizing different asteroid classes. They concluded that, with respect to spectral reflectance data, polarimetry provides a fully complementary approach to asteroid classification. The polarimetric properties of asteroids of various taxonomic classes were also derived and discussed in several more recent papers (Belskaya et al., 2005; Fornasier et al., 2006; Gil-Hutton, 2007; Gil-Hutton et al., 2008 , 2014; Gil-Hutton and Cañada-Assandri, 2011 , 2012; Cañada-Assandri et al., 2012). The main conclusion is that asteroids of the same taxonomic class as derived from spectral reflectance data, tend also to show similar polarimetric properties.

Here we complement previous analyses with new polarimetric data. Section 2 presents new observations of 15 main belt asteroids and their analysis. In Section 3 we discuss polarimetric properties of main asteroid classes and define a polarimetric classification for 283 main-belt asteroids.

2. Observations and results

Polarimetric observations of 15 main belt asteroids were carried out in 2005–2012. Table 1 presents the results of our polarimetric observations. For each asteroid observation, we list the epoch and mean time of observations in UT, the adopted filter, the phase angle α, the polarization degree P_r and the position angle θ_r in the coordinate system referring to the scattering plane as defined by Zellner and Gradie (1976), together with their root-mean-square errors σ_P and σ_θ. The last column refers to the observation site where observations were carried out.

In particular, the observations were carried out using different telescopes and instruments at four observational sites which we briefly characterized below.

Observations at the Asiago Observatory. Polarimetric observations were carried out using the polarimetric mode of the Faint Object Spectrographic Camera (AFOSC) mounted at the 1.8 m telescope of the Astrophysical Observatory of Asiago in Italy. The polarimeter allows simultaneous measurements of the polarized flux at angles 0, 45, 90, and 135° using a wedged double Wollaston prism (Oliva, 1997). These four beams are sufficient to determine the linear polarization parameters I, Q, and U with a single exposure. A polarimetric survey of asteroids at the Asiago telescope was made in 2002–2006. The results of most of the observations were published by Fornasier et al. (2006) where the description of the instrument, data acquisition and reduction was given. Here we present observations done in 2005–2006 which were not included in the above-mentioned paper. More recently, the Asiago polarimeter has been moved to the Nordic Optical Telescope (NOT) in La Palma (Canary Islands, Spain) and continued to be used for asteroid polarimetry (e.g. Fornasier et al., 2015).

Observations at the Crimean Astrophysical Observatory (CrAO). The observations were made in 2012 using the 1.25 m telescope of the Crimean Astrophysical Observatory equipped with a five-channel UBVRI photopolarimeter (Piirola, 1989). The method of observations and data processing have previously described in

details (see Shakhovskoy and Efimov 1972; Belskaya et al., 1987). Here we consider observations only in the R-band which was obtained with the best accuracy.

Observations at the Complejo Astronómico El Leoncito (CASLEO). For observations we use the 2.1 m telescope equipped with a double-hole aperture polarimeter. The polarimeter has rapid modulation provided by a rotating achromatic half-wave retarder and a Wollaston prism beam-splitter. The detailed description of the polarimeter, data acquisition and data reduction can be found in Gil-Hutton et al. (2008).

Observations at the LOIANO Observatory. Polarimetric observations were carried out in 2010–2012 at the Loiano station of the Astronomical Observatory of Bologna, Italy. We used the 1.52 m Cassini telescope equipped with Bologna Faint Object Spectrograph and Camera (BFOSC). The technical specifications of the instrument are given at http://www.bo.astro.it/loiano. The imaging polarimetry mode of the BFOSC is implemented with a Wollaston prism in the filter wheels and with the relative mask in the slit wheels. The prism gave strips of the images with orthogonal polarization of dimensions 1100×80 pixels, corresponding to about $10' \times 40''$. To measure the Stokes parameters, couple of images were recorded with the BFOSC in the standard position and another couple with the BFOSC rotated by 45°. We obtained sequence of images at the four angles, i.e. 0, 45, 90, and 135°.

All obtained polarization measurements were of a good quality (see errors in Table 1). In order to control instrumental polarization we measured two polarimetric standard stars with large and small polarizations each night. Observations of the same object obtained with different instruments are well consistent, indicating that the instrumental polarization was carefully corrected. Having at our disposal these new data we are now able to better characterize the polarization-phase behavior of the observed asteroids. We summarize the estimated polarimetric parameters of the measured asteroids in Table 2. The Table also includes diameters and albedos taken from Usui et al. (2013), and composition types according to Tholen (1984) and DeMeo et al. (2009).

The individual phase curves including both new and already published data for the observed asteroids are presented in Fig. 1. The data for asteroids (21) Lutetia and (64) Angelina are shown in Figs. 2–4. The data were fit to the so-called trigonometric function proposed by Lumme and Muinonen (1993) (see Section 3 for details) .We comment the results obtained for each target below.

(21) Lutetia. It was the target of the ESA Rosetta space mission fly-by on July 10th, 2010 (Sierks et al., 2011). Belskaya et al. (2010) found indications of possible variations of linear polarization over Lutetia's surface. These authors analyzed polarimetric observations of the asteroid performed in 1973–2008 at different telescopes (Zellner and Gradie, 1976; Fornasier et al., 2006; Gil-Hutton, 2007; Belskaya et al., 1987 , 2009, 2010) and noticed a scatter in the polarization phase curve exceeding observational errors. The analysis of the deviations of the polarization degree from the fit of the phase curve has shown systematic rather than random polarization variations probably correlated with asteroid rotation. To check this assumption we have performed new polarimetric observations of (21) Lutetia in March 16–18, 2010. Observations were aimed at studying possible variations of the polarization with the asteroid rotation. Simultaneously with polarimetric measurements we obtained photometric lightcurves in order to check for possible correlations.

The measured polarization degree and position angle of the polarization versus rotational phase are shown in Fig. 2. The lightcurve measured in the R band during our observations is also presented. The possible variations in polarization degree are about $\pm 0.1\%$, which do not exceed 2σ of our measurements. If these variations are real, they do not apparently correlate with the Lutetia's lightcurve.

Table 1
Results of polarimetric observations.

Asteroid	Date, UT	Band	α, deg	P_r, %	σ_P, %	θ_r, deg	σ_θ, deg	Telescope
21 Lutetia	2006 04 06.80	V	17.4	−0.72	0.07	76.0	2	Asiago
21 Lutetia	2010 03 16.84	R	5.46	−1.17	0.06	84.7	2	LOIANO
21 Lutetia	2010 03 17.82	R	5.86	−1.13	0.05	85.3	2	LOIANO
21 Lutetia	2010 03 18.88	R	6.26	−1.18	0.09	86.5	4	LOIANO
24 Themis	2011 09 21.88	R	0.54	−0.25	0.03	83	2	LOIANO
24 Themis	2011 09 22.90	R	0.89	−0.37	0.06	89	2	LOIANO
24 Themis	2011 09 23.97	R	1.22	−0.45	0.05	82	2	LOIANO
24 Themis	2011 09 29	V	3.0	−0.79	0.02	64.9	2	CASLEO
24 Themis	2011 09 30	V	3.3	−0.83	0.02	65.8	2	CASLEO
59 Elpis	2012 09 14.92	R	8.4	−1.48	0.08	88.4	2	CrAO
59 Elpis	2012 09 15.93	R	7.95	−1.11	0.07	86.5	2	CrAO
59 Elpis	2012 09 24.96	R	3.87	−0.92	0.07	86.2	2	CrAO
59 Elpis	2012 10 05.92	R	2.84	−0.61	0.06	89.8	3	CrAO
59 Elpis	2012 10 06.96	R	3.25	−0.59	0.09	88.2	4	CrAO
59 Elpis	2012 12 12.84	R	18.26	−0.16	0.07	77.5	10	CrAO
64 Angelina	2006 04 04.84	V	4.8	−0.23	0.07	80.2	2	Asiago
64 Angelina	2010 04 19.05	V	24.8	0.27	0.03	5.7	3	CASLEO
64 Angelina	2011 07 27.12	V	17.5	−0.07	0.02	112.8	8	CASLEO
64 Angelina	2012 08 28.90	V	1.0	−0.26	0.05	89	7	LOIANO
71 Niobe	2006 04 22.86	V	23.1	0.32	0.06	9.7	2	Asiago
71 Niobe	2011 07 28.04	V	26.3	0.59	0.02	21.8	1	CASLEO
87 Sylvia	2005 12 20.90	V	10.32	−0.95	0.04	84.3	2	Asiago
87 Sylvia	2010 09 04.14	V	13.7	−1.12	0.07	64.8	2	CASLEO
87 Sylvia	2011 07 28	V	18	−0.45	0.03	89	1	CASLEO
87 Sylvia	2011 09 29	V	6.2	−0.91	0.02	106.4	1	CASLEO
87 Sylvia	2011 09 30	V	5.9	−0.79	0.02	112.1	1	CASLEO
140 Siwa	2005 12 09.85	V	17.28	−0.93	0.05	94.4	1	Asiago
140 Siwa	2005 12 20.84	V	19.19	−0.61	0.07	81.1	2	Asiago
142 Polana	2005 12 10.99	V	9.33	−1.06	0.09	98.3	1	Asiago
142 Polana	2005 12 21.82	V	13.57	−0.60	0.06	77.6	1	Asiago
153 Hilda	2006 04 22.91	V	5.55	−0.97	0.05	92.1	2	Asiago
153 Hilda	2006 04 24.85	V	6.08	−0.95	0.05	92.4	2	Asiago
165 Loreley	2005 12 21.91	V	2.56	−0.83	0.06	93.5	1	Asiago
165 Loreley	2006 04 24.81	V	14.8	−0.74	0.09	89.4	2	Asiago
216 Kleopatra	2006 04 24.89	V	7.25	−0.92	0.08	92.5	2	Asiago
216 Kleopatra	2010 04 22.01	V	18.3	−0.07	0.06	145.1	3	CASLEO
234 Barbara	2005 12 09.91	V	15.83	−1.28	0.07	85.4	1	Asiago
234 Barbara	2005 12 20.95	V	18.57	−1.26	0.07	83.3	2	Asiago
289 Nenetta	2005 12 10.05	V	8.42	−0.44	0.12	89.4	1	Asiago
289 Nenetta	2005 12 20.98	V	12.9	−0.20	0.06	63.9	2	Asiago
503 Evelyn	2005 12 09.89	V	9.03	−0.95	0.06	86.0	1	Asiago
503 Evelyn	2005 12 20.92	V	13.95	−1.31	0.04	85.4	1	Asiago
503 Evelyn	2006 04 22.81	V	20.8	−0.41	0.06	85.8	2	Asiago
1021 Flammario	2006 04 22.93	V	7.6	−1.14	0.03	89.5	2	Asiago

We find also an indication of variations of the position angle of the polarization plane over Lutetia's surface. The position angle is systematically smaller than 90° for the surface seen between the primary minimum and the secondary maximum. Our observations were made close to the equatorial aspect. The aspect angle is estimated to be 109° assuming the pole coordinates $\lambda_0 = 56°$ and $\beta_0 = -6°$ (Carry et al., 2012). The deviations of the position angle of polarization from 90° for a part of the Lutetia's surface could be caused by large-scale surface irregularities seen for Lutetia from space images (Sierks et al., 2011).

The combined polarization-phase curve of asteroid (21) Lutetia is shown in Fig. 3. It includes our data and the data published by Zellner and Gradie (1976), Fornasier et al. (2006), Gil-Hutton (2007), Gil-Hutton et al. (2014), Belskaya et al. (1987, 2009, 2010). The scatter of the data over the fitted phase function exceeds the errors of individual measurements. We assume that these differences may be connected with the aspect of observations and caused by heterogeneous surface properties of Lutetia. Our observations indicate that possible variations of polarization over Lutetia's surface seen close to equatorial view do not exceed 0.1% in P_r and 10° in the position angle θ_r. Measurements with higher accuracy are needed to confirm and further investigate such possible effects.

(24) Themis. Asteroid (24) Themis with a diameter of $\sim$180 km is the largest member of the big Themis asteroid family located in the outer part of the asteroid belt at the heliocentric distance $\sim$3.2 au. This asteroid has a low albedo and is classified as C by Tholen (1984), and Ch by Fornasier et al. (2016). Campins et al. (2010) found evidence of the likely presence of water ice widespread on the surface, based on spectral reflectance data. Fornasier et al. (2016) suggested the possible presence of aqueously altered minerals. Previous polarimetric observations of Themis revealed a deep negative polarization branch with $P_{min} = -1.62\%$ at the phase angle $\alpha_{min} \sim 9°$ (Chernova et al., 1994). These observations were made down to the phase angle of 2.1°. Our new polarimetric observations reached smaller phase angles in order to measure the polarimetric behavior near opposition. The measured values of the polarization degree are plotted in Fig. 1 together with literature data (Chernova et al., 1994). The new and old measurements are in a good agreement within their accuracy. They show a usual polarization-phase angle behavior with polarization tending to decrease to zero approaching zero phase angle. This behavior does not differ from the polarization phase curve for other low albedo asteroids for which the signatures of ice were not found. Since polarimetry is sensitive to a presence of widespread water ice (see e.g. Dougherty and Geake, 1994) we can conclude
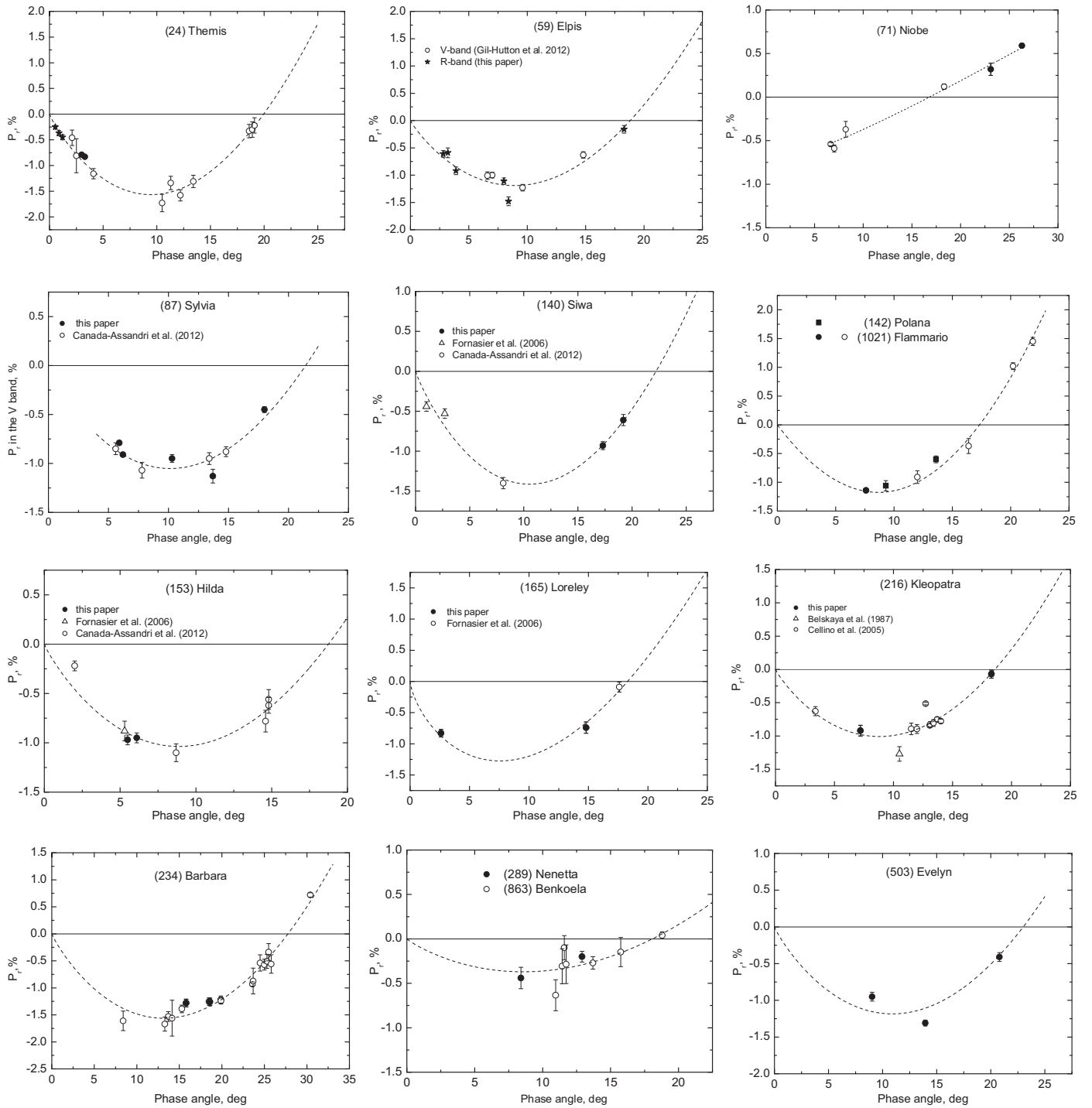
Fig. 1. The polarization-phase curve of the measured asteroids. New observations are shown by filled symbols and previously published data are shown by open symbols. Note that for asteroids (24) Themis and (59) Elpis we presents observations both in *V* (filled circles) and in *R* (filled stars) bands. The corresponding references to the published data for each asteroid are given in the text. The dashed lines shows the best fit of the Lumme and Muinonen function.

that it is hard to expect a large amount of water ice on Themis surface.

(59) Elpis. The large low-albedo asteroid (59) Elpis (D∼180 km) was classified as CP by Tholen (1984) and B by Bus and Binzel (2002). Shevchenko et al. (1996) found a peculiarity in the magnitude phase angle dependence of this asteroid, which shows linear trend down to small phase angles and does not exhibit any nonlinear opposition effect. The aim of our observations was to measure polarization-phase curve and search for possible correlation of

photometric and polarimetric effects. The polarization-phase curve of (59) Elpis (Fig. 1) which includes our observations in the R-band and also published measurements by Gil-Hutton et al. (2012) in the V-band is given in Fig. 1. The phase curve is characterized by the typical behavior for P-class asteroids (see Section 3.2).

(64) Angelina. It is an E-type asteroid showing a peculiar feature centered at 0.49 μm attributed to the presence of sulfides (Fornasier et al., 2008; Clark et al., 2004). Measurements of Zellner and Gradie (1976) covered the 6–24° phase angle range and re-

Table 2
Polarimetric parameters of the observed asteroids.

| Asteroid	Type	D, km	p_V	$|P_{min}|\%$	α_{inv} deg
(21) Lutetia	M, Xc	$121 \times 101 \times 75$[b]	0.19[b]	1.30 ± 0.10	24.0 ± 0.2
(24) Themis	C	177	0.08	1.57 ± 0.15	19.9 ± 0.2
(59) Elpis	CP, B[a]	156	0.05	1.25 ± 0.15	18.8 ± 0.6
(64) Angelina	E, Xe	54	0.52	0.31 ± 0.1	18.2 ± 0.9
(71) Niobe	S, Xe[a]	81	0.33	0.57 ± 0.1	16.7 ± 1.3
(87) Sylvia	P, X	263	0.04	1.1 ± 0.1	~ 20
(140) Siwa	P	111	0.07	1.4 ± 0.2	~ 22
(142) Polana	F	50	0.05	~ 1.1	~ 17
(153) Hilda	P, X	163	0.07	1.1 ± 0.15	–
(165) Loreley	CD	174	0.05	–	18.3 ± 0.5
(216) Kleopatra	M, Xe	122	0.15	1.1 ± 0.2	19 ± 1
(234) Barbara	S, L	48	0.19	1.56 ± 0.15	27.8 ± 0.3
(289) Nenetta	A	31	0.29	~ 0.5	–
(503) Evelyn	XC,Xe[a]	90	0.05	>1.4	~ 22–23
(1021) Flammario	F	97	0.05	1.2 ± 0.1	17.3 ± 0.5

[a] Bus and Binzel (2002).
[b] Sierks et al. (2011).
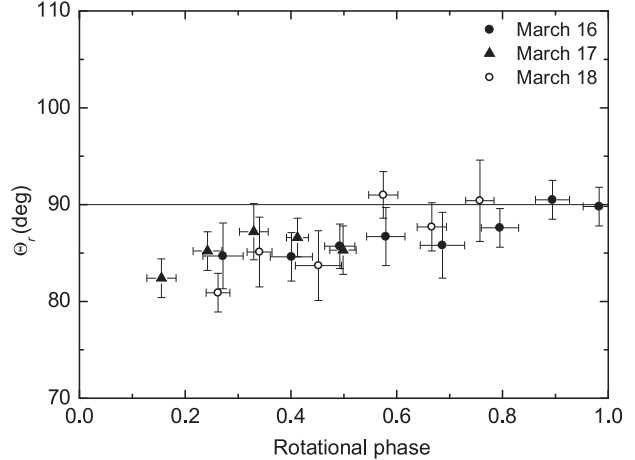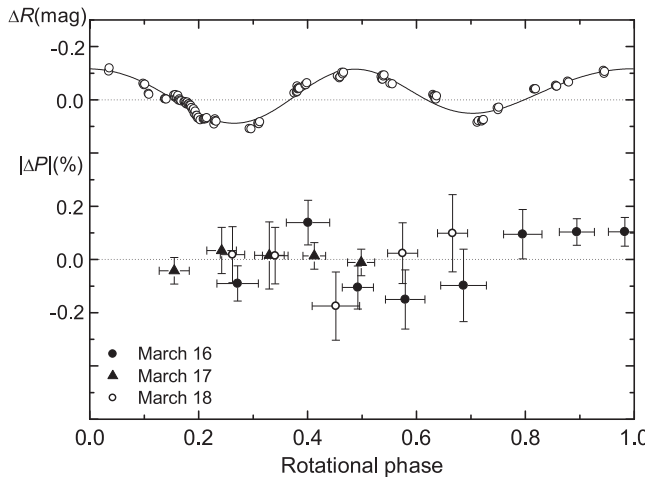
Fig. 2. Relative magnitude ΔR and polarization degree $\Delta P = P_r - P_{mean}$ (left) and the position angle of the polarization plane θ_r (right) versus rotational phase for (21) Lutetia.

vealed a shallow negative polarization branch with $P_{min} = -0.32\%$ and the inversion angle $\alpha_{inv} = 18.2°$ in the G filter (close to the V band). After discovery of a sharp brightness opposition effect of Angelina at $\alpha < 2°$ (Harris et al., 1989) several attempts were made to search for a sharp peak of negative polarization at small phase angles predicted by the coherent backscattering mechanism. Some 1994 observations (Kiselev et al., 1996) showed a positive polarization at $\alpha < 1.5°$, but they were later recognized as unreliable due to large background polarization of the full Moon (Rosenbush et al., 2005). Intensive measurements in UBVRI filters at $\alpha = 0.4$–13° were made in 1995, 1999, and 2000/2001 oppositions by Rosenbush et al. (2005). The authors claimed the discovery of a polarization opposition effect with an amplitude of $\sim -0.4\%$ centered at $\alpha_{min} \sim 1.8°$ superimposed to the regular negative polarization branch. They also found that the amplitude was apparition-dependent with a largest amplitude of about -0.5 to -0.7% in V-band in 1997 (Rosenbush et al., 2005). Later new observations of Angelina in 2008, 2011 and 2012 were published by Zaitsev et al. (2014). They analyzed together new and previously available observations and confirmed the presence of a polarization opposition effect in the form of a narrow secondary minimum at small phase angles. By fitting the available measurements of polarization degree they found two polarization minima at $\sim 1.5°$ and $\sim 7°$ (Zaitsev et al., 2014).

We observed Angelina in 2006 and 2010–2012 in the V band (see Table 1). Due to weather conditions we were not able to obtain a good phase angle coverage. The results of our observations are shown in Fig. 4 together with literature data obtained in the V and R bands (Zellner and Gradie, 1976; Rosenbush et al., 2005; Cañada-Assandri et al., 2012; Zaitsev et al., 2014). The data in the V and R bands can be considered together since spectral variations of negative polarization for E-type asteroids are rather weak (e.g. Bagnulo et al. 2015).

In a separate figure we plotted only the most accurate available measurements, having an associated error $\leq 0.05\%$. The presence of a secondary minimum at small phase angles is not seen when we consider only these data (Fig. 4). New data are well-consistent with the previous observations. There is no evidence on aspect-dependent variations of negative polarization degree of Angelina exceeding observation errors. The phase curve is well-fit by a polarization-phase function with $P_{min} = -0.3\%$, $\alpha_{min} \sim 5°$, and $\alpha_{inv} = 18.2°$.

(71) Niobe. The taxonomy of this asteroid is rather controversial. It was classified as S-type by Tholen (1984), but it was later attributed to the Xe class by Bus and Binzel (2002). The asteroid's size and albedo were estimated as $D = 93 \pm 1$ km, $p_v = 0.24 \pm 0.03$ (Masiero et al., 2011) and $D = 81 \pm 1$ km and $p_v = 0.33 \pm 0.01$ (Usui et al., 2013). It is the second largest member of the high inclination Gallia family (Nesvorny, 2012). It is not, however, recognized as a Gallia family member by Milani et al. (2014). Previous polarimetric measurements of Niobe have revealed substantially lower polarization as compared to most S-type asteroids (Fornasier et al., 2006).
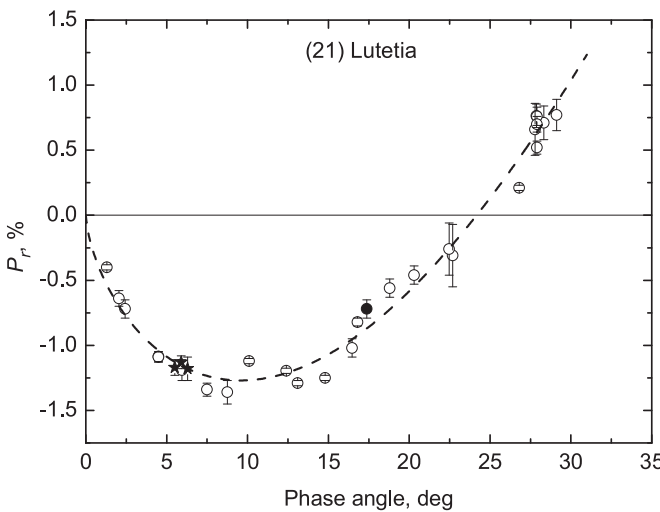
Fig. 3. The polarization-phase curve of (21) Lutetia. New observations are shown by black circles in the V band and by stars in the R band. Previously published measurements in the V band (Zellner and Gradie, 1976; Fornasier et al., 2006; Gil-Hutton, 2007; Gil-Hutton et al., 2014; Belskaya et al., 1987, 2009, 2010) are shown by open symbols. The dash line is the best-fit of the Lumme and Muinonen function.

Our new observations were aimed at measuring the polarimetric slope and at deriving the albedo of this asteroid. The polarization-phase curve of (71) Niobe including also previously published measurements (Zellner and Gradie, 1976; Fornasier et al., 2006; Gil-Hutton et al., 2014) is shown in Fig. 1. We obtained the following polarimetric parameters: h $= 0.056 \pm 0.003\%/°$, $\alpha_{inv} = 16.7 \pm 1.3°$, $P_{min} \sim -0.57\%$ at $\alpha_{min} \sim 7°$. Using the updated relationship of "polarimetric slope – albedo" (Cellino et al., 2015b) we have calculated the polarimetric albedo of $p_v = 0.34 \pm 0.08$ which is in a good agreement with the AKARI data (Usui et al., 2013). Polarimetric properties of (71) Niobe are similar to A-type asteroids. Further observations are needed to clear up surface composition of this asteroid.

(87) Sylvia. This large outer main-belt asteroid with a diameter of 263–288 km and a low albedo value of 4% (Masiero et al., 2011; Usui et al., 2013) was classified as a P-type by Tholen (1984). (87) Sylvia is the largest member of a collisional family and the

first triple system identified among asteroids. The diameters of the satellites were estimated to be of about 23 and 7 km (Berthier et al., 2014). We measured the polarization degree at five phase angles from 5.9 to 18°. The results are plotted in Fig. 1 together with the published measurements by Cañada-Assandri et al., (2012). The polarization curve is rather symmetric with $P_{min} = -1.1 \pm 0.1\%$ at $\alpha_{min} \sim 10°$ and the inversion angle $\alpha_{inv} \sim 20°$. The scatter of the observations around the best-fit polarization phase curve may indicate some possible variegation of the polarization degree of $\sim 0.1\%$. The polarimetric behavior is typical for a P-type asteroid (see Section 3.2).

(140) Siwa. This asteroid, having $D = 111$ km was classified as the P-type by Tholen (1984) and Cb-type by Lazzaro et al. (2004). It was intensively observed as it was selected as one of possible targets of the Rosetta space mission (Birlan et al., 2004). Previous polarimetric observations were published by Fornasier et al. (2006) and Canada-Assandri et al. (2012). They covered small phase angles. Our new measurements were made at larger phase angles in order to estimate the inversion angle. The polarization phase curve has rather deep negative branch with $P_{min} \sim -1.4\%$ at $\alpha_{min} \sim 10–12°$ and an inversion angle $\alpha_{inv} \sim 22°$. The negative branch is deeper as compared to other P-class asteroids (59) Elpis and (87) Sylvia (Fig. 1).

(142) Polana. This asteroid of $D = 50$ km was classified as F-type by Tholen (1984) and B-type by Bus and Binzel (2002). It is the largest member of the Polana family located in the inner asteroid belt. This family is mainly populated by low-albedo asteroids including several F-types (Cellino et al., 2001). Recently it was suggested that the so-called Nysa-Polana complex might include at least two low-albedo families of different age (Walsh et al., 2013). More recent spectroscopic observations by De Leon et al. (2016) do not strengthen this hypothesis. We present the first polarimetric measurements of this asteroid in the V band at two phase angles near the polarization minimum. They are shown in Fig. 1 and can be compared with the data for (1021) Flammario, another F-type asteroid in our dataset. The polarization phase curve morphology of these two objects seem to be rather similar with $P_{min} \sim -1.1\%$ and the inversion angle $\alpha_{inv} \sim 17°$. The inversion angle is small as is typically observed for F-type asteroids which are characterized by shallower negative polarization branch and smaller inversion angle compared to other low-albedo asteroids (Belskaya et al., 2005).

(153) Hilda. It is the largest member of the Hilda group orbiting in a 2:3 orbital resonance with Jupiter and having semi-major axis
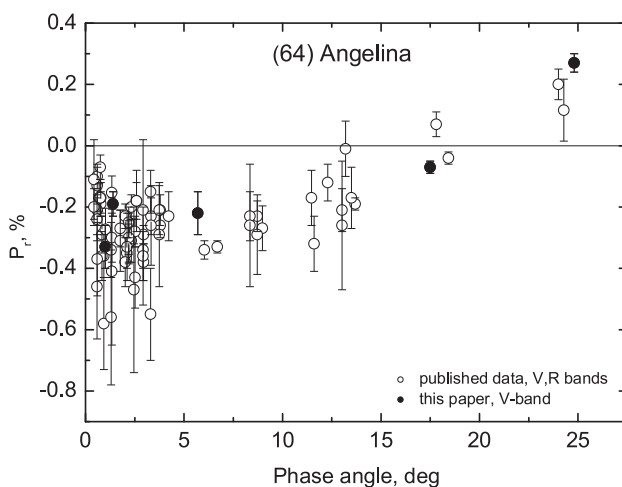

Fig. 4. The polarization-phase curve of (64) Angelina. New observations are shown by black circles. The left figure presents the published observations in the V and R bands (Zellner and Gradie, 1976; Rosenbush et al., 2005; Cañada-Assandri et al., 2012; Zaitsev et al., 2014). The right figure contains only those measurements which were made with an accuracy ≤0.05% in P_r.
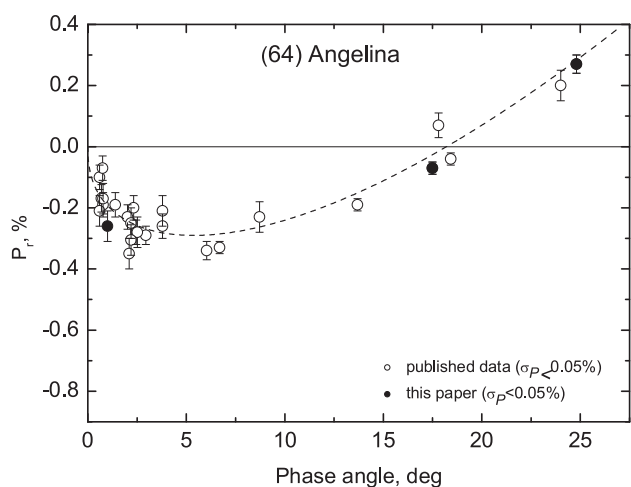
of 3.97 au. It was classified as the P-type by Tholen (1984) and X-type by Bus and Binzel (2002). Previous polarimetric observations were published by Fornasier et al. (2006) and Cañada-Assandri et al. (2012). Our new measurements made at two phase angles are in agreement with the literature data (Fig. 1). The negative branch with $P_{min} \sim -1.1\%$ at $\alpha_{min} \sim 7-9°$ is typical for the P-type asteroids.

(165) Loreley. It is a large main-belt asteroid of $D = 174$ km classified as the CD-type by Tholen (1984) and Cb-type by Bus and Binzel (2002). Previous polarimetric observations were obtained at a single phase angle of 16° by Fornasier et al. (2006). With our new measurements made at two phase angles it is possible to estimate an inversion angle $\alpha_{inv} \sim 18.3°$ The polarization-phase behavior (Fig. 1) is similar to that observed for C-type asteroids.

(216) Kleopatra. It is a dumbbell-shaped object with overall dimensions $127 \times 94 \times 81$ km derived from radar observations (Ostro et al., 2000). Its shape was confirmed by adaptive optics imaging which revealed the presence of two small satellites (Descamps et al., 2011). The asteroid was classified as the M-type (Tholen, 1984) and Xe-type (Bus and Binzel, 2002; Fornasier et al., 2010). The high density of Kleopatra estimated by Descamps et al. (2011) and a high radar albedo (Ostro et al., 2000) seem to confirm a highly metallic composition. Previous polarimetric observations were published by Belskaya et al. (1987) and Cellino et al. (2005). Our new measurements together with the published data allow to estimate $P_{min} \sim -1.1\%$ and $\alpha_{inv} \sim 19°$ (Fig. 1). Two measurements lay outside from the fitted curve which may indicate possible changes of polarization degree with rotation.

(234) Barbara. This asteroid initially classified as S (Tholen, 1984) was later attributed to the L-class (DeMeo et al., 2009). Cellino et al. (2006) discovered the unusual polarimetric behavior of (234) Barbara characterized by an extraordinarily wide negative polarization branch with the largest inversion angle ever observed for asteroids. Later several other asteroids sharing this property were found and called "Barbarians" (see Cellino et al., 2015a for a review). We measured the polarization degree at two phase angles and found a good agreement with previously published data (Cellino et al., 2006; Gil-Hutton et al., 2014). The inversion angle is estimated to be as large as 27.8°

(289) Nenetta. This asteroid has an estimated diameter of $D = 31$ km and $p_v = 0.29$ (Usui et al., 2013). It belongs to the rare A taxonomic class (Tholen, 1984; Bus and Binzel, 2002). We obtained the first polarimetric observations of this asteroid at two phase angles and we found that $P_{min} \sim -0.5\%$. These data are in agreement with the available data for another A-type asteroid (863) Benkoela (Cellino et al., 2005; Fornasier et al., 2006). The data for these two A-type asteroids are plotted together in Fig. 1.

(503) Evelyn. This asteroid, with $D = 90$ km and $p_v = 0.05$ (Usui et al., 2013), was classified as a Ch object (Bus and Binzel, 2002). Our measurements at three phase angles are the first polarimetric observations of this asteroid. The inversion angle is expected to be rather large $\alpha_{inv} \sim 22-23°$ which is typical of Ch-type asteroids. The data show dispersion and cannot be well-fit to the Lumme and Muinonen phase function. The measurement at $\alpha = 9°$ is outside of the average phase curve for Ch asteroid. Further observations are needed to understand whether such peculiarity is real.

(1021) Flammario. This asteroid of 98 km in diameter belongs to the rare F-class. Previous polarimetric observations were published by Fornasier et al. (2006) and Gil-Hutton et al. (2012). Our new V measurements were made at a single phase angle close to polarization minimum. The polarization phase curve is shown in Fig. 1 together with the data for the other F-type asteroid (142) Polana. The estimated polarimetric parameters $P_{min} \sim -1.2 \pm 0.1\%$ at $\alpha_{min} \sim 9 \pm 1°$ and the inversion angle $\alpha_{inv} \sim 17.3 \pm 0.5°$ are typical for the F class (see Belskaya et al., 2005).

3. Analysis and discussion

We have analyzed all data available today on asteroid polarimetry. They include the data presented in the Asteroid Polarimetric Database (APD) at the Small Bodies Node of the Planetary Data System (Lupishko, 2014), in the Torino database (Cellino et al., 2005), and the data from the papers which were not yet included in the APD (Gil-Hutton et al., 2014; Zaitsev et al., 2014; Cellino et al., 2014; Bagnulo et al., 2016, and the present paper). We focus here on the analysis of negative polarization branch and we do not consider near-Earth asteroids observed at large phase angles. We looked through all data and selected the measurements in the V and R filters, and also in the G-filter which is close to the V filter (Zellner and Gradie, 1976). The expected spectral dependence of linear polarization in the considered phase angle range ($<30°$) and wavelength range (0.55–0.66 μm) are rather small (see Belskaya et al., 2009; Bagnulo et al., 2015), so we think that merging together V and R data should not introduce significant errors. We consider only those measurements of linear polarization having an accuracy $\leq 0.2\%$ (with a few exceptions for $P_r \geq 2\%$ for which $\sigma \leq 0.3\%$ was accepted). The final data-set includes measurements for 337 asteroid, but more or less good sampling of phase angles are available for less than 90 objects.

We computed best-fit of the data for individual objects observed at several phase angles by using both the so-called trigonometrical and the linear-exponential functions. The trigonometrical function proposed by Lumme and Muinonen (1993) has the following form:

$$P(\alpha) = b \sin^{c_1}\alpha \cos^{c_2}\frac{1}{2}\alpha \sin(\alpha - \alpha_0),$$

where the parameter b and the inversion angle α_0 are considered as free parameters, while c_1 and c_2 can be fixed. The main advantage of the function is that it gives physically reasonable behavior of the polarization phase dependence in a wide range of phase angles. According to Lumme and Muinonen (1993) the parameter c_2 equals to 0.35 for various bodies (asteroids, comets, satellites), while the parameter c_1 takes a value of 0.7 for asteroids. Most part of available data for asteroids are well-fit using two free parameters. The effect of parameters of this function on shapes of phase curves was analyzed by Pentilla et al. (2005).

The exponential-linear function (Kaasalainen et al., 2003; Muinonen et al., 2009) has the following form:

$$P_r = A(e^{-\alpha/B} - 1) + C \cdot \alpha$$

where α is the phase angle expressed in degrees, and A, B, and C are free parameters.

Both functions provide similar fits in the cases of a good phase angle coverage up to $\alpha \leq 30°$. For sparse data the estimated values of P_{min} and α_{inv} depend on the chosen function. With only few measurements for an individual object the uncertainties in polarimetric parameters are quite large. We found only 77 asteroids for which both P_{min} and α_{inv} can be reliably estimated from individual phase curves. The data for all other asteroids were analyzed by fitting combined phase curve for asteroids belonging to the same compositional types.

3.1. Relationship P_{min}-inversion angle

The relationship between the two parameters characterizing the negative polarization branch P_{min} and α_{inv} has been considered in the past as diagnostic of the surface texture (e.g. Dollfus et al., 1989). This conclusion was based on laboratory measurements of meteorites and silicate rocks, that found different width of the negative polarization branches for bare rocks, coarse and fine-grained samples (Geake and Dollfus, 1986; Dollfus et al., 1989).
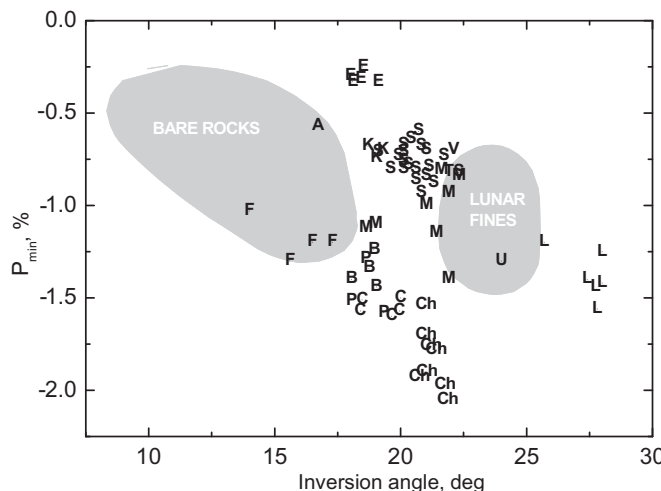
Fig. 5. Relationship between P_{min} vs. α_{inv} for asteroids of different taxonomic types. The domains for bare rocks and lunar fines as indicated by Dollfus et al. (1989) are also shown.

In Fig. 5 we presented an updated plot P_{min} vs. α_{inv} for 77 asteroids with reliable polarimetric parameters. Asteroids are displayed using letters corresponding to their published taxonomic classes (Tholen, 1984; DeMeo et al., 2009). The domains for bare rocks and lunar fines according to Dollfus et al. (1989) are also indicated. The range of inversion angles inherent for asteroid surfaces extends now from the domain of bare rock to the domain of fines and beyond (see Fig. 5). Asteroids of the same class tend clearly to group together. This suggests that the location of asteroids in this plot is primarily related to differences in surface composition rather than to substantial variations in the surface texture from dust free surface to very small-grained regolith.

By taking into account various taxonomic classifications (Tholen, 1984; Bus and Binzel, 2002; DeMeo et al., 2009) we found that asteroids belonging to the Ch, F, S, L, E classes are well-distinguished by their polarization properties. Asteroids of the M-type in Tholen's classification or Xk, Xc in DeMeo et al. (2009) taxonomy are spread in the P_{min} vs. α_{inv} plot, suggesting the presence of relevant differences among asteroids belonging to these classes. We found only small differences in the polarimetric properties of C, P and B objects, whereas a part of B-asteroids (DeMeo et al., 2009) which had been previously classified as F by Tholen (1984) display particular properties. Asteroids belonging to the K and L classes which are the end-members of the S-class display distinct polarimetric behaviors. Asteroids of rare classes such as A and V tend to occupy particular places at the plot P_{min} vs. α_{inv}.

3.2. Polarization properties of the main asteroid classes

We have plotted the combined polarization phase curves for main compositional types of asteroids. For the purpose we consider only those asteroids for which classifications are unambiguous and compatible in various taxonomic schemes (Tholen, 1984; Bus and Binzel, 2002; DeMeo et al., 2009). We obtained average polarization-phase dependence for a particular compositional type. The data were fitted by both trigonometric and linear-exponential functions. We used the least square method to determine the best fit to the data weighted with the inverse of the error of individual measurement. The differences between two fits were negligible but we used both functions since the first one directly gives an inversion angle α_{inv}. and the second function directly gives the value of polarimetric slope h. The value of P_{min} was determined as the mean minimal value of both fits. The parameters determined for

each compositional type are presented in Table 3. This Table includes the mean values of polarimetric parameters, their standard deviations, and the list of asteroids which were considered for each type. The mean geometric albedos calculated using the WISE and AKARI catalogs are also given for each class.

Average polarization-phase curves are shown in Fig. 6 for low (a), moderate (b) and high (c) albedo taxonomic types. The figure shows distinctly different polarimetric behavior for different asteroid classes. Moreover, asteroids of similar albedos (e.g. P and F, K and L, A and V types) may have different polarization curves.

The trend of increasing values of P_{min} (in absolute value) for decreasing albedo is not strictly respected (Table 3) which is in contradiction to the well-known empirical relationship "P_{min} – albedo" used for determination of asteroid albedos (see Cellino et al., 2015b). For the darkest asteroids belonging to the F, P, D-types P_{min} (in absolute value) is smaller compared to the value found for B, C, and Ch types (see Table 3 and Fig. 6). The explanation can be that we observe the so-called "saturation" effect discovered in the laboratory for very dark surfaces (Zellner et al., 1977). The depth of negative polarization increases when albedo decreases down to ∼6% but any further decrease of albedo results in a weakening of negative polarization which is well-seen in Fig. 6. This effect has been observed for the F-type asteroids (Belskaya et al., 2005) and D-type objects (Bagnulo et al., 2016). One of the possible explanations is that the regolith microstructure of these asteroids optically more homogeneous than of other classes of low albedo asteroids (Belskaya et al., 2005).

Thus, the geometric albedo does not seem to play a dominant role in determining the polarization–phase behavior at phase angles near P_{min}. As shown in laboratory experiments the correlation of P_{min} with albedo may be destroyed by the interplay of the different physical parameters of the surfaces (Shkuratov et al., 2002). We confirm therefore that using P_{min} for determination of asteroid's albedo should be taken with much caution, as already recommended by Cellino et al. (2015b). In some cases it can be difficult to distinguish even between low and moderate albedo surfaces.

The observed similarity of the polarization phase curves for asteroids belonging to the same taxonomic class (derived from spectral reflectance data) suggest that polarimetric behavior is intimately related to surface composition. Polarimetric properties are therefore very useful for the purposes of asteroid taxonomy, e.g. to distinguish several types of asteroids which are difficult to distinguish based on spectral data alone.

3.3. Classification of asteroids from polarimetric data

Low-albedo classes. Polarimetric properties of the F-type asteroids are completely different from other classes due to their unusually small inversion angles (Fig. 6). The most distinctive spectral feature of the F class as compared to other asteroid types is an absence of UV absorption (see Tholen, 1984). Recent classifications based on asteroid spectra which do not cover UV wavelengths did not separate the F type (Bus and Binzel, 2002; DeMeo et al., 2009). Asteroids previously classified as *F* belong today mostly to the *B* or C classes. Polarimetry gives a way to separate F-type from other low-albedo types. In the future, spectral data obtained by the Gaia satellite, covering also the blue part of the spectrum, will be used to produce a new asteroid taxonomy and it will be interesting to see whether the old F class will be identified again. Polarimetric data will be essential for the scientific validation of the Gaia-based taxonomy (Cellino and Dell'Oro, 2012).

Low-albedo asteroids with large UV dropoff which were classified as G-type by Tholen (1984) and showing the hydrated silicates absorption band centered at about 0.7 μm have been recently classified in the Ch and Cgh classes (Bus and Binzel, 2002; DeMeo et al., 2009). These last types show distinctly different polarization

Table. 3
Mean polarization parameters of asteroids of different composition types in the V-band.

| Type	p_V	$|P_{min}|$, %	α_{min}, deg	α_{inv}, deg	h, %/deg	Asteroids
Ch	0.072 ± 0.016	1.85 ± 0.10	9.0 ± 1.0	21.3 ± 0.1	0.440 ± 0.050	13, 19, 41, 48, 51, 54, 141, 410, 654
C	0.065 ± 0.015	1.55 ± 0.55	8.7 ± 2.1	19.4 ± 0.1	0.387 ± 0.037	1, 10, 24, 31, 93, 128, 147, 165, 210, 324, 444, 466, 511, 566
P	0.057 ± 0.013	1.24 ± 0.35	8.8 ± 2.1	19.2 ± 0.2	0.601 ± 0.225	46, 56, 59, 76, 87, 140, 153
B	0.083 ± 0.034	1.41 ± 0.35	8.2 ± 2.1	19.1 ± 0.2	0.307 ± 0.021	2, 47, 85, 88, 213, 253, 372
F	0.058 ± 0.011	1.15 ± 0.10	7.5 ± 1.7	15.7 ± 0.2	0.608 ± 0.193	142, 268, 302, 335, 419, 704, 1021
D	0.047 ± 0.008	1.15 ± 0.15	7.8 ± 1.5	18.2 ± 0.3	0.341 ± 0.109	269. 322, 588,732, 944, 1583, 2797, 4543, 6545, 21,601
M	0.184 ± 0.052	1.00 ± 0.25	9.0 ± 2.0	21.5 ± 0.2	0.193 ± 0.012	16, 22, 55, 69, 75, 97, 110, 125, 129, 132, 135, 161, 184, 201, 216, 224, 250, 325, 337, 338, 347, 369, 382, 441, 516, 558, 757, 849
S	0.235 ± 0.046	0.75 ± 0.20	8.0 ± 1.2	20.7 ± 0.2	0.110 ± 0.005	5, 6, 7, 14, 17, 18, 20, 23, 25, 27, 29, 30, 40, 67, 73, 113, 115, 124, 138, 158, 170, 183, 197, 204, 219, 288, 341, 351, 456, 550, 787, 832
K	0.172 ± 0.044	0.90 ± 0.15	8.7 ± 1.2	19.6 ± 0.2	0.253 ± 0.041	15, 42, 89, 114, 186, 221, 472
L	0.157 ± 0.039	1.43 ± 0.20	12.9 ± 1.5	28.0 ± 0.2	0.438 ± 0.164	172, 234, 236, 387, 402, 679, 980
Q	0.29 ± 0.08	> 0.5		19.0 ± 1.1	0.078 ± 0.010	214,869
A	0.345 ± 0.180	0.5 ± 0.1	5 ± 2	18.2 ± 1.6	0.049 ± 0.008	246, 289, 354, 863, 1600
V	0.34	0.68 ± 0.05	6.5 ± 1.0	21.7 ± 0.2	0.061 ± 0.003	4
E	0.508 ± 0.094	0.35 ± 0.05	5 ± 1	18.4 ± 0.4	0.039 ± 0.003	44, 64, 214, 317, 434, 2867
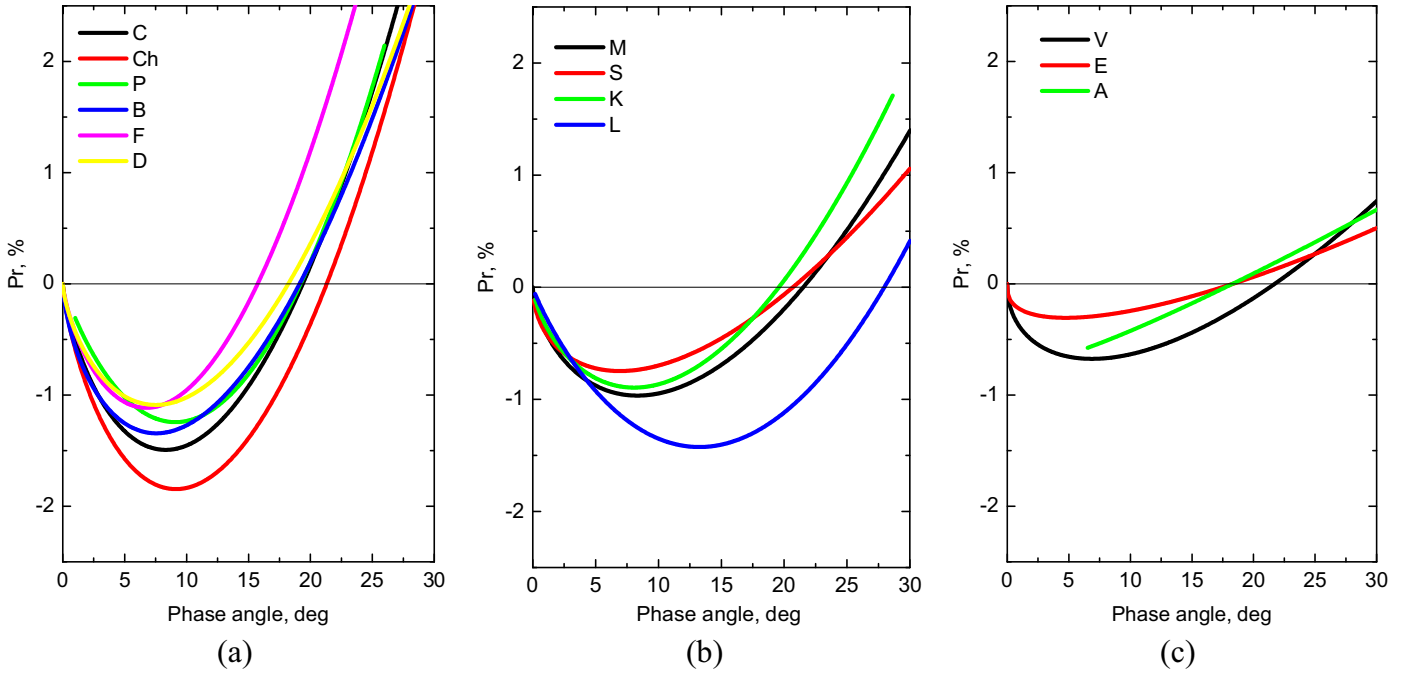
Fig. 6. Average fits of the polarization-phase curves are shown for low (a), moderate (b) and high (c) albedo taxonomic types.

behavior compared to other classes, characterized by the deepest negative polarization branches (Fig. 6).

Asteroids of the C and P classes have similar inversion angles but different depth of negative polarization which can be used to distinguish between them. D-type asteroids show the smallest depth of negative polarization like F-asteroids, but larger inversion angles.

Moderate-albedo classes. Asteroids of the S-complex have rather similar polarimetric properties. Among 75 asteroids which were classified as S in one or more classifications only 8 asteroids reveal systematic deviations from the mean polarization curve exceeding observational errors. Asteroids (9) Metis, (18) Melpomene, (29) Amphitrite, (189) Phthia, and (230) Athamantis show deeper negative branch, while (138) Tolosa, (169) Zelia, and (542) Susanna are characterized by a shallower negative polarization branches compared to the average behavior of the S class. Most probably, the above-mentioned asteroids are end-members of the S-type population and they deserve a more careful classification. Asteroids (9) Metis and (29) Amphitrite were classified by Bus and Binzel (2002) as the T and L types, respectively, but this classification

was not confirmed by DeMeo et al. (2009), who took into account also spectral reflectance data in the near IR. The only Q-type object measured at the phase angles smaller than inversion angle is the near-Earth asteroid (214869) 2007 PA8 (Fornasier et al., 2015). It is characterized by the inversion angle a bit smaller than a typical value for the S-asteroids (see Table 3).

Asteroids of K- and L-types show different polarization curves and can be distinguished on the basis of polarimetric behavior alone (Fig. 6). Deep negative branch with extremely large inversion angle is a distinct feature of the majority of measured L-type asteroids. In fact, all asteroids classified as L-type by DeMeo et al. (2009) for which polarization measurements are available show $\alpha_{inv} \sim 26$–$28°$. On the other hand, all measured K-type asteroids from DeMeo et al. (2009) show usual polarization-phase curves with an inversion angle $\sim 20°$. Some of these asteroids were put by Bus and Binzel (2002) into different classes (i.e., L as K or K as L), due to the fact that the corresponding differences in spectral reflectance at visible wavelengths are rather weak for these classes. Large differences in polarization behaviors of L and K classes suggest different surface properties (in composition and/or regolith

properties) in spite of rather small spectral differences. Polarimetric measurements of L and K candidates close to the inversion angle give a unique way to reliably distinguish between these two types. K-type asteroids have deeper P_{min} and smaller inversion angle compared to S-type asteroids. The only exception in our sample is (15) Eunomia classified as K by DeMeo et al. (2009) and as S by Bus and Binzel (2002) which shows polarimetric properties typical for the S-type asteroids.

The M-type asteroids from Tholen's classification have deeper and wider negative polarization branch compared to the S- and K-type asteroids (Fig. 6). Their polarimetric properties are well-distinguished from low- and high albedo types giving a way to refine the classification of X, Xk, Xe, Xc-type asteroids from Bus and Binzel (2002) and DeMeo et al. (2009). Indeed, using the polarimetric measurements we can easily distinguish X-complex asteroids in low (P), moderate (M) and high (E) albedo types following previously adopted classification of Tholen (1984).

High-albedo classes. The measured E-type asteroids show very similar polarization phase-angle behaviors. There are no differences within the errors of measurements ($\leq 0.05\%$) between EII and EIII types as defined in Fornasier et al. (2008).

The diversity within the rare A class is evident. Asteroid (246) Asporina shows a smaller inversion angle compared to (863) Benkoela and (1600) Vyssotsky. These objects also differ in albedos and in spectral properties. Asteroid (246) Asporina is characterized by the lack of a 2 μm feature while for (863) Benkoela this feature was detected (Sanchez et al., 2014). Polarimetric data revealed heterogeneity within the A-class and can be useful in distinguishing sub-classes among olivine-rich objects. Two asteroids, (71) Niobe and (152) Atala, for which previous classifications by Tholen (1984) and Bus and Binzel (2002) were inconsistent (S, Xe for Niobe and D, S for Atala), show polarimetric properties similar to A-type asteroids.

The V-type asteroid (4) Vesta has a wider negative polarization branch compared to E and A-classes (see Table 3).

Polarimetric classifications of asteroids is given in Table 4. It contains 283 main belt asteroids for which composition type from polarimetric observations can be estimated. We marked in a bold font the asteroids which show deviations from the previous classification. For 32 asteroids we gave several possible classes since the available polarimetric data are not enough to distinguish between classes. For the majority of the considered asteroids their spectral classification was confirmed, but in the cases of specific classes such as F, B, X, K, L-classes it was also refined. There are less than 10% asteroids in our sample for which polarimetric properties noticeably deviate from the average polarization phase curve of the corresponding type. We marked such asteroids as U in Table 4. These asteroids can be interesting targets for more detailed investigation in order to understand their polarimetric peculiarities. For asteroids (77) Frigga, (216) Kleopatra, (217) Eudora, and (503) Evelyn, there are considerable scatter of some measurements from the fitted curves which may indicate possible variations of the polarization degree over the surface or erroneous data.

4. Conclusions

We have presented new polarimetric observations of 15 main belt asteroids of different composition types. Polarimetric observations of asteroid (21) Lutetia, one of the Rosetta targets, revealed possible variations of the position angle of the polarization plane over the surface. Analysis of new and published observations of the E-type asteroid (64) Angelina demonstrated that the possible existence of a secondary minimum at small phase angles suggested by some authors (Rosenbush et al., 2005; Zaitsev et al., 2014) disappears when we limit our analysis only to the most accurate available measurements of linear polarization ($\leq 0.05\%$).

Table 4
Polarimetric classification of asteroids.

Asteroid		Type		
		Polari-metric	Tholen	DeMeo
1	Ceres	C	G	C
2	Pallas	B	B	B
3	Juno	S	S	Sq
4	Vesta	V	V	V
5	Astraea	S	S	S
6	Hebe	S	S	–
7	Iris	S	S	S
8	Flora	S	S	Sw
9	**Metis**	SU	S	–
10	Hygiea	C	C	C
11	Parthenope	K/S	S	Sq
12	Victoria	S	S	–
13	Egeria	Ch	G	Ch
14	Irene	S	S	S
15	Eunomia	S/K	S	K
16	Psyche	M	M	Xk
17	Thetis	S	S	S
18	**Melpomene**	SU	S	S
19	Fortuna	Ch	G	Ch
20	Massalia	S	S	S
21	**Lutetia**	U	M	Xc
22	Kalliope	M	M	X
23	Thalia	S	S	–
24	Themis	C	C	C
25	Phocaea	S	S	S
27	Euterpe	S	S	S
29	**Amphitrite**	SU	S	S
30	Urania	S	S	S
31	Euphrosyne	C	C	–
34	Circe	C	C	Ch
37	Fides	S	S	S
39	Laetitia	S	S	Sqw
40	Harmonia	S	S	S
41	Daphne	Ch	C	Ch
42	Isis	K	S	K
43	Ariadne	S	S	Sq
44	Nysa	E	E	–
46	Hestia	P	P	–
47	**Aglaja**	B	C	–
48	Doris	Ch	CG	Ch
49	Pales	Ch	CG	Ch
50	Virginia	Ch	X	Ch
51	Nemausa	Ch	CU	Cgh
52	Europa	C	CF	C
54	Alexandra	Ch	C	Cgh
55	Pandora	M	M	Xk
56	Melete	P	P	Xk
58	**Concordia**	C?	C	Ch
59	Elpis	P	CP	–
62	**Erato**	Ch	BU	–
63	Ausonia	S	S	Sw
64	Angelina	E	E	Xe
67	Asia	S	S	S
68	Leto	S	S	–
69	Hesperia	M	M	Xk
70	Panopaea	Ch	C	Cgh
71	**Niobe**	A	S	–
72	**Feronia**	Ch/C	TDG	–
73	Klytia	S	S	S
75	Eurydike	M	M	–
76	Freia	P	P	C
77	Frigga	MU	MU	Xe
78	Diana	Ch	C	Ch
84	Klio	Ch	G	Ch
85	**Io**	B	FC	C
87	Sylvia	P	P	X
88	**Thisbe**	B	CF	–
89	Julia	K	S	–
90	Antiope	C	C	C
91	Aegina	Ch/C	CP	–
92	Undina	M	X	Xk
93	Minerva	C	CU	C
95	Arethusa	Ch	C	–

(continued on next page)

Table 4 (*continued*)

Asteroid		Type		
		Polari-metric	Tholen	DeMeo
97	**Klotho**	MU	M	Xc
98	Ianthe	Ch/C	CG	–
102	**Miriam**	CU	P	–
104	**Klymene**	C?	C	–
105	Artemis	Ch	C	Ch
106	Dione	Ch	G	Cgh
110	Lydia	M	M	Xk
113	Amalthea	S	S	–
114	Kassandra	K	T	K
115	Thyra	S	S	S
118	Peitho	S	S	–
122	Gerda	K	ST	–
124	Alkeste	S	S	–
125	Liberatrix	M	M	–
126	Velleda	S	S	–
128	Nemesis	C	C	C
129	Antigone	M	M	–
130	Elektra	Ch	G	Ch
131	Vala	K	SU	K
132	Aethra	M	M	Xe
133	Cyrene	S	SR	S
134	Sophrosyne	Ch	C	–
135	Hertha	M	M	–
138	**Tolosa**	SU	S	–
139	Juewa	P	CP	–
140	Siwa	P	P	–
141	Lumen	Ch	CPF	–
142	Polana	F	F	–
147	Protogeneia	C	C	C
150	Nuwa	C/B	CX	C
152	**Atala**	A?	I	–
153	Hilda	P	P	X
154	Bertha	C/B	–	–
158	Koronis	S	S	S
160	Una	C/P	CX	Xk
161	Athor	M	M	–
165	Loreley	C	CD	–
169	**Zelia**	SU	S	–
170	Maria	S	S	S
172	Baucis	L	S	–
183	Istria	S	S	–
184	Dejopeja	M	X	–
186	Celuta	K	S	–
188	Menippe	S	S	S
189	**Phthia**	SU	S	–
192	Nausikaa	S	S	Sw
195	Eurykleia	Ch	C	–
197	Arete	S	S	–
200	Dynamene	Ch	C	–
201	Penelope	M	M	Xk
204	Kallisto	S	S	–
208	Lacrimosa	K/S	S	–
210	Isabella	C	CF	Cb
213	**Lilaea**	B	F	–
214	Aschera	E	E	Cgh
216	Kleopatra	M	M	Xe
217	Eudora	P?	X	–
219	Thusnelda	S	S	–
221	Eos	K	S	K
224	Oceana	M	M	–
226	Weringia	K/S	–	S
230	**Athamantis**	SU	S	–
233	Asterope	P?	T	Xk
234	Barbara	L	S	L
236	Honoria	L	S	L
237	Coelestina	S	S	Sr
238	Hypatia	C?	C	–
243	Ida	S	S	Sw
246	Asporina	A	A	A
250	Bettina	M	M	Xk
253	Mathilde	B	–	–
259	Aletheia	P	CP	–
268	Adorea	F	FC	–
269	Justitia	D	–	D

Table 4 (*continued*)

Asteroid		Type		
		Polari-metric	Tholen	DeMeo
273	Atropos	K	SCTU	–
276	Adelheid	P	X	–
284	Amalia	Ch	CX	–
288	Glauke	S	S	S
289	Nenetta	A	A	A
302	Clarissa	F	F	–
305	Gordonia	S	S	–
308	Polyxo	T?	T	T
317	Roxane	E	E	–
322	Phaeo	D	X	D
324	Bamberga	C	CP	–
325	Heidelberga	M	M	–
335	Roberta	F	FP	–
337	Devosa	M	X	Xk
338	Budrosa	M	M	–
339	Dorothea	K	S	–
341	California	S	S	–
347	Pariana	M	M	–
349	Dembowska	A?	R	R
350	Ornamenta	Ch	C	–
351	Yrsa	S	S	–
354	Eleonora	A	S	A
357	Ninina	C/B	CX	–
359	Georgia	M	CX	Xk
365	**Corduba**	C	X	–
367	Amicitia	S	–	–
368	**Haidea**	U	D	–
369	Aeria	M	M	–
372	Palma	B	BFC	–
374	Burgundia	S	S	–
376	Geometria	S	S	–
377	**Campania**	Ch/C	PD	–
381	**Myrrha**	B	C	–
382	Dodona	M	M	–
384	Burdigala	S	S	–
386	Siegena	C	C	–
387	Aquitania	L	S	L
396	Aeolia	M/P?	–	–
397	**Vienna**	T/L?	S	–
399	Persephone	M	–	–
400	Ducrosa	B	–	–
402	Chloe	L	S	L
404	**Arsinoe**	B	C	–
406	Erna	P	P	–
409	Aspasia	C	CX	–
410	Chloris	Ch	C	–
412	Elisabetha	P	–	–
419	Aurelia	F	F	–
420	Bertholda	P	P	–
431	Nephele	B	B	–
434	Hungaria	E	E	Xe
438	**Zeuxo**	B	F:	–
441	Bathilde	M	M	–
443	Photographica	S	S	–
444	Gyptis	C	C	C
449	Hamburga	C	C	–
451	**Patientia**	B	CU	–
456	Abnoba	S	–	S
458	Hercynia	L	S	–
466	Tisiphone	C	C	–
471	Papagena	S	S	–
472	Roma	K	S	–
476	Hedwig	P	P	–
478	Tergeste	K	S	–
481	Emita	Ch	C	–
487	Venetia	K	S	–
502	Sigune	S	S	–
503	**Evelyn**	Ch	XC	–
504	Cora	M	–	–
511	Davida	C	C	–
516	Amherstia	M	M	–
532	Herculina	S	S	S
542	**Susanna**	SU	S	–
550	Senta	S	S	–

Table 4 (*continued*)

Asteroid		Type		
		Polari-metric	Tholen	DeMeo
554	Peraga	C/B	FC	–
558	Carmen	M	M	–
564	Dudu	C/P/B	CDX:	–
566	Stereoskopia	C	C	–
572	Rebekka	M/U	XDC	–
579	Sidonia	K	S	K
584	Semiramis	S	S	–
600	Musa	S	–	–
602	Marianna	C	C	–
616	Elly	L/K	S	–
620	Drakonia	E	E	–
625	Xenia	S	–	Sw
654	Zelinda	Ch	C	–
660	Crescentia	S	S	–
661	Cloelia	K	S	K
662	Newtonia	S/K	–	–
678	Fredegundis	M	–	–
679	Pax	L	I	L
690	Wratislavia	B	CPF	–
694	**Ekard**	Ch	CP:	–
702	Alauda	P/C	C	–
704	Interamnia	F	F	–
732	Tjilaki	D	–	–
737	Arequipa	S	S	–
739	Mandeville	P	X	Xc
753	Tiflis	S	S	–
757	Portlandia	M	XF	–
762	**Pulcova**	B	F	–
779	Nina	M	–	–
785	**Zwetana**	U	M	Cb
787	Moskva	S	–	–
796	Sarita	M	XD	–
832	Karin	S	–	S
838	Seraphina	P	P	–
849	Ara	M	M	–
857	**Glasenappia**	S	MU	–
863	Benkoela	A	A	A
897	Lysistrata	K	S	–
925	Alphonsina	S	S	S
944	Hidalgo	D	D	D
980	Anacostia	L	SU	–
1021	Flammario	F	F	–
1025	**Riema**	M	E	–
1099	Figneria	K	–	–
1105	**Fragaria**	U/L	ST	–
1146	Biarmia	M	X	–
1166	Sakuntala	S	–	–
1251	Hedera	E	E	–
1453	Fennia	K	S	–
1509	Esclangona	K	S	–
1600	Vyssotsky	A	–	–
1659	Punkaharju	S	–	S
1727	Mette	S	S	–
2131	Mayall	S	S	–
2577	Litva	S	EU	–
2867	Steins	E	–	–
3169	**Ostro**	B	TS	–
3447	Burckhalter	E	–	–
3906	Chao	Ch/L/U	–	–
4116	Elachi	S	–	–
6249	Jennifer	M?	–	–

Using new and previously published data we determined polarimetric parameters of individual asteroids and the mean polarimetric parameters of the main composition classes. We found that the majority of asteroids measured so far show polarimetric behavior very close to the average polarization phase curve found for the corresponding taxonomic class. There are less than 10% asteroids whose polarimetric properties noticeably deviate from the average polarization phase curve. Asteroids of the same taxonomic class have a tendency to cluster in the plot P_{min} vs α_{inv}, i.e. to have similar polarization-phase behavior. This suggests that the relationship between two parameters characterizing the negative polarization branch P_{min} and α_{inv} may be primarily related to surface composition rather than to substantial variations in the surface texture from dust free surface to very small-grained regolith as was considered early. Moreover, the geometric albedo does not seem to play a dominant role in determining the polarization–phase behavior near polarization minima. The determination of asteroid's albedo based on P_{min} should be taken with a caution.

We have shown that using polarimetric data it is possible to refine asteroid taxonomy and produce a polarimetric classification for 283 main belt asteroids. The polarimetric data allow to distinguish among low, moderate and high-albedo types within the X-complex, and Ch, F, L, K objects characterizing by particular polarimetric properties.

Acknowledgments

References

Bagnulo, S., Cellino, A., Sterzik, M., 2015. Linear spectro-polarimetry: a new diagnostic tool for the classification and characterisation of asteroids. MNRAS Lett. 446, L11–L15.

Belskaya, I.N., Lupishko, D.F., Shakhovskoy, N.M., 1987. Negative polarization spectra for five asteroids. Soviet Astron. Lett. 13, 219–220.

Belskaya, I.N., Shevchenko, V.G., Kiselev, N.N., Krugly, Y.N., Shakhovskoy, N.M., Efimov, Y.S., Gaftonyuk, N.M., Cellino, A., Gil-Hutton, R., 2003. Opposition polarimetry and photometry of S- and E-type asteroids. Icarus 166, 276–284.

Belskaya, I.N., Shkuratov, Y.G., Efimov, Y.S., Shakhovskoy, N.M., Gil-Hutton, R., Cellino, A., Zubko, E.S., Ovcharenko, A.A., Bondarenko, S.Y., Shevchenko, V.G., Fornasier, S., Barbieri, C., 2005. The F-type asteroids with small inversion angles of polarization. Icarus 178, 213–221.

Belskaya, I.N., Levasseur-Regourd, A.C., Cellino, A., Efimov, Y.S., Shakhovskoy, N.M., Hadamcik, E., Bendjoya, P., 2009. Polarimetry of main belt asteroids: wavelength dependence. Icarus 199, 97–105.

Belskaya, I.N., Fornasier, S., Krugly, Y.N., Shevchenko, V.G., Gaftonyuk, N.M., Barucci, M.A., Fulchignoni, M., 2010. Puzzling asteroid 21 Lutetia: our knowledge prior to the Rosetta fly-by. Astron. Astrophys. 515, A29.

Belskaya, I., Cellino, A., Gil-Hutton, R., Muinonen, K., Shkuratov, Y., et al., 2015. Asteroid polarimetry. In: Michel, P., et al. (Eds.), Asteroids IV. University of Arizona, Tucson, pp. 151–163.

Berthier, J., Vachier, F., Marchis, F., Durech, J., Carry, B., 2014. Physical and dynamical properties of the main belt triple asteroid (87) Sylvia. Icarus 239, 118–130.

Birlan, M., Barucci, M.A., Vernazza, P., Fulchignoni, M., Binzel, R.P., Bus, S.J., Belskaya, I., Fornasier, S., 2004. Near-IR spectroscopy of asteroids 21 Lutetia, 89 Julia, 140 Siwa, 2181 Fogelin, and 5480 (1989 YK8), potential targets of the Rosetta mission, remote observations campaign on IRTF. New Astron. 9 (N5), 343–351.

Bus, S.J., Binzel, R.P., 2002. Phase II of the small main-belt asteroid spectroscopic survey. a feature-based taxonomy. Icarus 158, 146–177.

Campins, H., Hargrove, K., Pinilla-Alonso, N., et al., 2010. Water ice and organics on the surface of the asteroid 24 Themis. Nature 464, 1320–1321.

Cañada-Assandri, M., Gil-Hutton, R., Benavidez, P., 2012. Polarimetric survey of main-belt asteroids. III. Results for 33 X-type objects. Astron. Astrophys. 542, A11.

Carry, B., Kaasalainen, M., Merline, W.J., et al., 2012. Shape modeling technique KOALA validated by ESA Rosetta at (21) Lutetia. Planet. Sp. Sci. 66, 200–212.

Clark, B.E., Bus, S.J., Rivkin, A.S., Shepard, M.K., Shah, S., 2004. Spectroscopy of X-type asteroids. Astron. J. 128, 3070–3081.

Cellino, A., Gil Hutton, R., Tedesco, E.F., Di Martino, M., Brunini, A., 1999. Polarimetric observations of small asteroids: preliminary results. Icarus 138, 129–140.

Cellino, A., Zappalà, V., Doressoundiram, A., Di Martino, M., Bendjoya, P., Dotto, E., Migliorini, F., 2001. The puzzling case of the Nysa–Polana family. Icarus 152, 225–237.

Cellino, A., Gil-Hutton, R., di Martino, M., Bendjoya, Ph., Belskaya, I.N., Tedesco, E.F., 2005. Asteroid polarimetric observations using the Torino UBVRI photopolarimeter. Icarus 179, 304–324.

Cellino, A., Belskaya, I.N., Bendjoya, P., Di Martino, M., Gil-Hutton, R., Muinonen, K., Tedesco, E.F., 2006. The strange polarimetric behavior of asteroid (234) Barbara. Icarus 180, 565–567.

Cellino, A., Dell'Oro, A., 2012. The derivation of asteroid physical properties from Gaia observations. Planet. Sp. Sci. 73, 52–55.

Cellino, A., Bagnulo, S., Tanga, P., Novakovic, B., Delbò, M., 2014. A successful search for hidden Barbarians in the Watsonia asteroid family. MNRAS 439, L75–L79.

Cellino, A., Gil-Hutton, R., Belskaya, I., 2015a. Polarimetry of asteroids. In: Kolokolova, L., Levasseur-Regourd, A.-C., Hough, J. (Eds.). In: Polarimetry of Stars and Planetary Systems, 20. Cambridge University Press, Cambridge, U.K, pp. 360–378.

Cellino, A., Bagnulo, S., Gil-Hutton, R., Tanga, P., Cañada-Assandri, M., Tedesco, E.F., 2015b. On the calibration of the relation between geometric albedo and polarimetric properties for the asteroids. MNRAS 451, 3473–3488.

Cellino, A., Bagnulo, S., Gil-Hutton, R., Tanga, P., Cañada-Assandri, M., Tedesco, E.F., 2016. A polarimetric study of asteroids: fitting phase-polarization curves. MNRAS 455 (2), 2091–2100.

Chernova, G.P., Lupishko, D.F., Shevchenko, V.G., 1994. Photometry and polarimetry of the asteroid 24 Themis. Kinematika Fiz. Nebesn. Tel, Tom 10 (2), 45–49.

De Leòn, J., Pinilla-Alonso, N., Delbò, M., Campins, H., Cabrera-Lavers, A., Tanga, P., Cellino, A., Bendjoya, P., Gayon-Markt, J., Licandro, J., Lorenzi, V., Morate, D., Walsh, K.J., DeMeo, F., Landsman, Z., Ali-Lagoa, V., 2016. Visible spectroscopy of the Polana family complex: spectral homogeneity. Icarus 266, 57–75.

DeMeo, F.E., Binzel, R.P., Slivan, S.M., Bus, S.J., 2009. An extension of the bus asteroid taxonomy into the near-infrared. Icarus 202, 160–180.

Descamps, P., Marchis, F., Berthier, J., et al., 2011. Triplicity and physical characteristics of asteroid (216) Kleopatra. Icarus 211, 1022–1033.

Dollfus, A., Wolff, M., Geake, J.E., Lupishko, D.F., Dougherty, L.M., 1989. Photo-polarimetry of asteroids. In: Binzel, R.P., Gehrels, T., Matthews, M.S. (Eds.), Asteroids II. University Arizona Press, Tucson, pp. 594–616.

Dougherty, L.M., Geake, J.E., 1994. Polarization by frost formed at very low temperatures, as relevant to icy planetary surfaces. Mon. Not. R. Astron. Soc. 271, 343–354.

Fornasier, S., Beskaya, I.N., Shkuratov, Y.G., Pernechele, C., Barbieri, C., Giro, E., Navasardyan, H., 2006. Polarimetric survey of asteroids with the Asiago telescope. Astron. Astrophys. 455, 371–377.

Fornasier, S., Migliorini, A., Dotto, E., Barucci, M.A., 2008. Visible and near infrared spectroscopic investigation of E-type asteroids, including 2867 Steins, a target of the Rosetta mission. Icarus 196 (1), 119–134.

Fornasier, S., Clark, B.E., Dotto, E., Migliorini, A., Ockert-Bell, M., Barucci, M.A., 2010. Spectroscopic survey of M-type asteroids. Icarus 210 (2), 655–673.

Fornasier, S., Beskaya, I.N., Perna, D., 2015. The potentially hazardous asteroid 2007 PA8: an unweathered L chondrite analogue surface. Icarus 250, 280–286.

Fornasier, S., Lantz, C., Perna, D., Campins, H., Barucci, M.A., Nesvorny, D., 2016. Spectral variability on primitive asteroids of the Themis and Beagle families: space weathering effects or parent body heterogeneity? Icarus 269, 1–14.

Geake, J.E., Dollfus, A., 1986. Planetary surface texture and albedo from parameter plots of optical polarization data. MNRAS 218, 75–91.

Gil-Hutton, R., 2007. Polarimetry of M-type asteroids. Astron. Astrophys. 464, 1127–1132.

Gil-Hutton, R., Mesa, V., Cellino, A., Bendjoya, Ph., Peñaloza, L., Lovos, F., 2008. New cases of unusual polarimetric behavior in asteroids. Astron. Astrophys. 482, 309–314.

Gil-Hutton, R., Cañada-Assandri, M., 2011. Polarimetric survey of main-belt asteroids. I. Results for fifty seven S-, L-, and K-type objects. Astron. Astrophys. 529, A86.

Gil-Hutton, R., Cañada-Assandri, M., 2012. Polarimetric survey of main-belt asteroids. II. Results for 58 B- and C-type objects. Astron. Astrophys. 539 A115.

Gil-Hutton, R., Cellino, A., Bendjoya, Ph., 2014. Polarimetric survey of main-belt asteroids. IV. New results from the first epoch of the CASLEO survey. Astron. Astrophys. 569, 6 id.A122.

Goidet-Devel, B., Renard, J.B., Levasseur-Regourd, A.-C., 1995. Polarization of asteroids. Synthetic curves and characteristic parameters. Planet. Space Sci 43, 779–786.

Harris, A.W., Young, J.W., Contreiras, L., Dockweiler, T., Belkora, L., Salo, H., Harris, W.D., Bowell, E., Poutanen, M., Binzel, R.P., Tholen, D.J., Wang, S., 1989. Phase relations of high albedo asteroids: the unusual opposition brightening of 44 Nysa and 64 Angelina. Icarus 81, 365–374.

Kaasalainen, S., Piironen, J., Kaasalainen, M., Harris, A.W., Muinonen, K., Cellino, A., 2003. Asteroid photometric and polarimetric phase curves: empirical interpretation. Icarus 161, 34–46.

Kiselev, N.N., Shakhovskoy, N.M., Efimov, Y.S., 1996. On the polarization opposition effect of E-type asteroid 64 Angelina. Icarus 120, 408–411.

Lazzaro, D., Angeli, C.A., Carvano, J.M., Mothé-Diniz, T., Duffard, R., Florczak, M., 2004. S ^{3}OS ^{2}: the visible spectroscopic survey of 820 asteroids. Icarus 172 (1), 179–220.

Lumme, K., Muinonen, K., 1993. A two-parameter system for linear polarization of some solar system objects. In: IAU Symposium 160, Asteroids, Comets, Meteors, Abstract, p. 194.

Lupishko, D.F., Mohamed, R.A., 1996. A new calibration of the polarimetric albedo scale of asteroids. Icarus 119, 209–213.

Lupishko D. F. 2014. Asteroid polarimetric database V8.0. NASA planetary data system, EAR-A-3-RDR-APD-POLARIMETRY-V8.0.

Masiero, J.R., Mainzer, A.K., Grav, T., et al., 2011. Main belt asteroids with WISE/NEOWISE. I. Preliminary albedos and diameters. Astrophys. J. 741, 20 id. 68.

Milani, A., Cellino, A., Knežević, Z., Novaković, B., Spoto, F., Paolicchi, P., 2014. Asteroid families classification: exploiting very large datasets. Icarus 239, 46–73.

Muinonen, K., Penttilä, A., Cellino, A., Belskaya, I.N., Delbò, M., Levasseur-Regourd, A.C., Tedesco, E.F., 2009. Asteroid photometric and polarimetric phase curves: joint linear-exponential modeling. Meteorit. Planet. Sci. 44, 1937–1946.

Nesvorny D., 2012. Nesvorny HCM Asteroid Families V2.0. NASA Planetary Data System, EAR-A-VARGBDET-5-NESVORNYFAM-V2.0.

Oliva, T., 1997. Wedged double Wollaston, a device for single shot polarimetric measurements. Astron. Astrophys. 123, 589–592.

Ostro, S.J., Hudson, R.S., Nolan, M.C., et al., 2000. Radar observations of asteroid 216 Kleopatra. Science 288 (5467), 836–839.

Penttilä, A., Lumme, K., Hadamcik, E., Levasseur-Regourd, A.-C., 2005. Statistical analysis of asteroidal and cometary polarization phase curves. Astron. Astrophys. 432, 1081–1090.

Piirola, V., 1989. Simultaneous five-color (UBVRI) photopolarimeter. In: Coyne, G.V., Magalhaes, A.M., Moffat, A.F.J., Schulte-Ladbeck, R.E., Tapia, S., Wickramasinghe, D.T. (Eds.), Polarized Radiation of Circumstellar Origin. University of Arizona Press, Tucson, pp. 735–746.

Rosenbush, V.K., Kiselev, N.N., Shevchenko, V.G., Jockers, K., Shakhovskoy, N.M., Efimov, Y.F., 2005. Polarization and brightness opposition effects for the E-type asteroid 64 Angelina. Icarus 178, 222–234.

Sanchez, J.A., Reddy, V., Kelley, M.S., et al., 2014. Olivine-dominated asteroids: mineralogy and origin. Icarus 228, 288–300.

Shakhovskoy, N.M., Efimov, Y.S., 1972. Polarization observations of nonstable stars and extragalactic object. I: Equipment, method of observation and reduction. Izv. Krymskoi Astrofiz. Obs. 45, 90–110.

Shevchenko, V.G., Chiorny, V.G., Kalashnikov, A.V., Krugly, Y.N., Mohamed, R.A., Velichko, F.P., 1996. Magnitude-phase dependences for three asteroids. Astron. Astrophys. Suppl. Ser. 115, 475–479.

Shkuratov, Y., Ovcharenko, A., Zubko, E., Miloslavskaya, O., Nelson, R., Smythe, W., Muinonen, K., Piironen, J., Rosenbush, V., Helfenstein, P., 2002. The opposition effect and negative polarization of structurally simulated planetary regoliths. Icarus 159, 396–416.

Sierks, H., Lamy, P., Barbieri, C., 2011. Images of asteroid 21 Lutetia: a remnant planetesimal from the early solar system. Science 334 (6055), 487–490.

Tholen, D., 1984. Asteroid Taxonomy from Cluster Analysis of Photometry Ph. D. thesis. University of Arizona.

Tholen, D.J., Barucci, M.A., 1989. In: Binzel, R.P., Gehrels, T., Matthews, M.S. (Eds.), Asteroids II. University of Arizona Press, Tucson, AZ, p. 298.

Usui, F., Kasuga, T., Hasegawa, S., Ishiguro, M., Kuroda, D., M¨uller, T.G., Ootsubo, T., Matsuhara, H., 2013. Albedo properties of main belt asteroids based on the all-sky survey of the infrared astronomical satellite AKARI. Ap. J. 762 article id. 56.

Walsh, K.J., Delbó, M., Bottke, W.F., Vokrouhlický, D., Lauretta, D.S., 2013. Introducing the Eulalia and new Polana asteroid families: re-assessing primitive asteroid families in the inner main belt. Icarus 225 (1), 283–297.

Zaitsev, S.V., Kiselev, N.N., Rosenbush, V.K., Kolesnikov, S.V., Antonyuk, K.A., 2014. Polarimetry of the E-type asteroid 64 Angelina. Kinemat. Phys. Celestial Bodies 30 (3), 155–160.

Zellner, B., Gradie, J., 1976. Minor planets and related objects. XX. Polarimetric evidence for the albedos and compositions of 94 asteroids. Astron. J. 81, 262–280.

Zellner, B., Lebertre, T., Day, K., 1977. The asteroid albedo scale – II. Laboratory polarimetry of dark carbon-bearing silicates. In: Proceedings of the Lunar Science Conference, vol. 8, pp. 1111–1117.